Prediction of the operating point of dendrites growing under coupled thermo-solutal control at high growth velocity

A.M. Mullis[†]

Institute for Materials Research, University of Leeds, Leeds LS2-9JT, UK.

Abstract

We use a phase-field model for the growth of dendrites in dilute binary alloys under coupled thermo-solutal control to explore the dependence of the dendrite tip velocity and radius of curvature upon undercooling, Lewis number (ratio of thermal to solutal diffusivity), alloy concentration and equilibrium partition coefficient. Constructed in the quantitatively valid thin-interface limit the model uses advanced numerical techniques such as mesh adaptivity, multigrid and implicit time-stepping to solve the non-isothermal alloy solidification problem for materials parameters that are realistic for metals. From the velocity and curvature data we estimate the dendrite operating point parameter, σ^*. We find that σ^* is non-constant and, over a wide parameter space, displays first a local minimum followed by a local maximum as the undercooling is increased. This behaviour is contrasted with a similar type of behaviour to that predicted by simple marginal stability models to occur in the radius of curvature, on the assumption of constant σ^*.

PACS: 81.30.Fb, 64.70.dm, 02.60.Lj, 05.70.Fh

[†] e-mail: A.M.Mullis@leeds.ac.uk; tel: +44 113 343 2568; fax: +44 113 343 2384.

1. INTRODUCTION

Dendritic solidification has been a subject of enduring interest within the scientific community, both because dendrites are a prime example of spontaneous pattern formation and due to their pervasive influence on the engineering properties of metals. As dendrites are self-similar when scaled against the tip radius, ρ, the ability to accurately predict ρ is a problem of central importance to the theory of dendritic growth. However, the difficulty in theoretically calculating ρ has been apparent since Ivantsov [1] showed that an isothermal paraboloid of revolution, growing at velocity V into its parent melt, undercooled by an amount ΔT, was a shape preserving solution to the diffusion equation, thus giving rise to the idea of the parabolic needle dendrite. The analytical solution for such a crystal is degenerate in that it relates the Peclet number, and not the growth velocity, to undercooling, where the Peclet number is defined as

$$Pt = \frac{V\rho}{2\alpha} \tag{1}$$

where α is the thermal diffusivity in the melt. Consequently, at a given undercooling an infinite set of solutions are admissible, subject to the condition $V\rho =$ constant. Such degeneracy is not observed in nature, where a well defined growth velocity can always be associated with a given undercooling, thus sparking the search for an additional mechanism to set the length scale, ρ, for the dendrite.

One of the most enduring solutions to this problem is based on a linear stability analysis of a plane solidification front against the growth of small perturbations [2]. This theory postulates that the dendrite grows at the largest value of ρ which is stable against the growth of such perturbations, as these would cause the tip to split hence reduce ρ, This is termed the limit of marginal stability. The principal prediction of this theory is that capillary forces break the Ivantsov degeneracy via the relationship

$$\rho^2 V = \frac{2\alpha d_o}{\sigma^*} \tag{2}$$

where d_o is a capillary length. σ^* is the so-called stability constant, which for a plane interface is given by Mullins & Sekerka [2] as $\sigma^* = 1/(4\pi^2) \approx 0.0253$.

This theory, particularly in its more sophisticated forms due to Lipton, Glicksman & Kurz (LGK) [3, 4] and Lipton, Kurz & Trivedi (LKT) [5], was reasonably successful in fitting experimentally determined velocity-undercooling data [6]. Moreover, direct simultaneous measurement of V and ρ for succinonitrile [7] yields an experimental value for σ^* in this system of 0.0195, in close agreement with the theory. However, despite this, there is no theoretical basis for the marginal stability hypothesis and agreement with experiment, such as it is, must be considered fortuitous. In particular, boundary integral methods [8, 9] (microscopic solvability theory) have shown that the Ivantsov equations have no solution in the absence of crystalline anisotropy, and that therefore the apparent agreement between marginal stability theory and experiment is fortuitous. The full analysis reveals that an equation similar to the one arising from marginal stability is encountered but that σ^* is the anisotropy-dependant eigenvalue for the problem which, in the limit of low Peclet numbers, is found to vary as $\sigma^*(\varepsilon) \propto \varepsilon^{7/4}$, where ε is a measure of the anisotropy strength.

In recent years further progress has been made towards understanding solidification phenomena [10] by the advent of by phase-field modelling [11, 12, 13], particularly through the formulation of the 'thin interface model', due to Karma & Rappel [14]. In the thin-interface model, asymptotic expansions of the solution on the solid and liquid sides of the boundary are matched such that a solution is obtained which is independent of the length scale chosen for the mesoscopic diffuse interface width. As a consequence of this the thin-interface model is capable of giving quantitatively correct predictions for V and ρ during dendritic growth, from which a back-calculation of σ^* may be undertaken in order to compare

with earlier stability-based theories. Interestingly, where calculation of σ^* has been undertaken away from the limit of vanishing Peclet number, both phase-field [15, 16] and numerical solvability [17, 18] models show that σ^* has not only a materials dependence, through the anisotropy strength, ε, but also a dependence upon the growth conditions. Specifically, for both the thermally controlled solidification of a pure substance [15, 16] and the (slow) isothermal solidification of an alloy [19], σ^* appears to decreases linearly with increasing Peclet number. Moreover, in the limited number of cases where phase-field models have been applied to alloy systems solidifying under coupled thermo-solutal control [19, 20, 21, 22], σ^* has been found to vary with undercooling, alloy concentration and Lewis number (= ratio of thermal to solutal diffusivity, α/D), with this variation in some cases being non-monotonic. The variation of σ^* with concentration appear to be borne out experimentally, with a re-evaluation by Li & Beckermann [23] of the data of Chopra *et al*. [24] for the transparent succinonitrile-acetone system showing a variation in σ^* with concentration of between a factor of 2 and 4 depending upon the undercooling considered.

This potentially makes the estimation of σ^* extremely problematic. Moreover, this is not simply an academic problem. As pointed out be Rebow & Browne [25], the stability constant is an intrinsic part of many alloy solidification models, including cellular automaton [26, 27], front-tracking [28] and one-domain multiphase models of both the volume [29, 30] and ensemble [31] averaging types. In general such models have tended to use (either explicitly or implicitly) the analytical value of σ^* as given by marginal stability theory, although in principal other values, either calculated or experimentally estimated [25], could also be used. This offers the possibility that such rule based models can to some extent be tuned to the specific material system being simulated and, given the linear dependence found between Peclet number and σ^* for systems under both pure thermal or pure solutal control, even to the local growth conditions. However, the complex, non-monotonic variation

observed in σ^* with increasing undercooling means that for alloy systems solidifying far from equilibrium where thermal effects cannot be ignored, estimating the value of σ^* without detailed and computationally expensive calculations is not possible.

In this paper we use a phase-field model of coupled thermo-solutal solidification to significantly extend our previous analysis of the variation of σ^* as a function of undercooling, presenting new data in which the effect of varying alloy concentration, Lewis number, and equilibrium partition coefficient, k_E, are systematically investigated. The model is based upon the equations presented by Ramirez & Beckermann [19, 20], but we use advanced numerical techniques such as local mesh adaptivity, implicit time-stepping and a multigrid solver to obtain solutions over a much wider parameter space than that explored by Ramirez & Beckermann. The model is formulated in the thin-interface limit [32], wherein the solutions are independent of the width of the diffuse interface and are therefore quantitatively valid.

It is found that σ^* shows a dependence upon all of the variables investigated, this being, to the best of our knowledge, the first time that it has been demonstrated that σ^* shows any dependence upon k_E. A model is proposed which accounts, at least qualitatively, for all of the functional dependencies observed in the behaviour of σ^*.

2. DESCRIPTION OF THE MODEL

The model adopted here is based upon that of [20] in which, following non-dimensionalization against characteristic length and time scales, W_0 and τ_0, the evolution of the phase-field, ϕ, and the dimensionless concentration and temperature fields U and θ are given by

$$A^2(\psi)\left[\frac{1}{Le}+Mc_\infty\left[1+(1-k_E)U\right]\right]\frac{\partial\phi}{\partial t}=\nabla\cdot\left(A^2(\psi)\nabla\phi\right)+\phi(1-\phi^2)$$
$$-\lambda(1-\phi^2)^2(\theta+Mc_\infty U)-\frac{\partial}{\partial x}\left(A(\psi)A'(\psi)\frac{\partial\phi}{\partial y}\right)+\frac{\partial}{\partial y}\left(A(\psi)A'(\psi)\frac{\partial\phi}{\partial x}\right) \quad (3)$$

$$\left(\frac{1+k_E}{2}-\frac{1-k_E}{2}\phi\right)\frac{\partial U}{\partial t}=\nabla\cdot\left(D\frac{1-\phi}{2}\nabla U+\frac{1}{2\sqrt{2}}\left|1+(1-k_E)U\right|\frac{\partial\phi}{\partial t}\frac{\nabla\phi}{|\nabla\phi|}\right)$$
$$+\frac{1}{2}\left(\left|1+(1-k_E)U\right|\frac{\partial\phi}{\partial t}\right) \quad (4)$$

$$\frac{\partial\theta}{\partial t}=\alpha\nabla^2\theta+\frac{1}{2}\frac{\partial\phi}{\partial t} \quad (5)$$

where, for 4-fold growth, $A(\psi) = 1 + \varepsilon.\cos(4\psi)$, ψ being the angle between the outward pointing normal to the solid-liquid interface and the principal growth direction, L and c_p are the latent and specific heats respectively and λ is a coupling parameter given by $\lambda = D/a_2 = a_1 W_0/d_0$ with a_1 and a_2 taking the values $5\sqrt{2}/8$ and 0.6267 respectively [32]. U and θ are related to physical concentration, c, and temperature, T, via

$$U=\frac{1}{1-k_E}\left(\left(\frac{2c/c_\infty}{1+k_E-(1-k_E)\phi}\right)-1\right) \text{ and } \theta=\frac{\Delta T-mc_\infty}{L/c_p}\ , \quad (6)$$

where m is the slope of the liquidus line, which has dimensionless form

$$M=\frac{|m|(1-k_E)}{L/c_p} \quad (7)$$

The governing equations are discritized using a finite difference approximation based upon a quadrilateral, non-uniform, locally-refined mesh with equal grid spacing in both directions. This allows the application of standard second order central difference stencils for the calculation of first and second differentials, while a compact 9-point scheme has been

used for Laplacian terms, in order to reduce the mesh induced [33] anisotropy. To ensure sufficient mesh resolution around the interface region and to handle the extreme multi-scale nature of the problem local mesh refinement (coarsening) is employed when the weighted sum of the gradients of ϕ, U and θ exceeds (falls below) some predefined value.

It has been shown elsewhere that if an explicit temporal discretization scheme is used for this problem the maximum stable time-step is given by $\Delta t \leq Ch^2$, where h is the minimum mesh spacing and $C = C(\lambda, Le, \Delta T)$, with C varying from ≈ 0.3 at $Le = 1$ to $C \leq 0.001$ at $Le = 500$ [34], leading to unfeasibly small time-steps at high Lewis number. Consequently, an implicit temporal discretization is employed here based on the second order Backward Difference Formula with variable time-step.

When using implicit time discretization methods it is necessary to solve a very large, but sparse, system of non-linear algebraic equations at each time-step. Multigrid methods are among the fastest available solvers for such systems and in this work we apply the non-linear generalization known as FAS (full approximation scheme [35]). The local adaptivity is accommodated via the multilevel algorithm originally proposed by Brandt [36]. The interpolation operator is bilinear while injection is used for the restriction operator. For smoothing the error we use a fully-coupled nonlinear weighted Gauss-Seidel iteration where the number of pre- and post-smoothing operations required for optimal convergence is determined empirically. Full details of the numerical scheme are given in [34, 37].

We obtain from the model the two key parameters characteristic of dendritic growth, namely the velocity and radius of curvature of the tip. The latter we obtain by fitting a parabolic profile to the $\phi = 0$ isoline using a 4^{th} order interpolation scheme described in [21, 34], as this has generally been felt [19, 38] to be more directly comparable to analytical dendrite growth theories [5], than the curvature obtained directly from the derivatives of ϕ at the tip.

In order to compare our results with analytical theories for the solidification of deeply undercooled alloys it is also useful to be able to calculate the equivalent radius selection parameter, σ^*, by using the values of V and ρ obtained directly from the phase-field model. For a model with only a single diffusing species, either heat in the case of the thermally controlled growth of a pure material or solute in the case of the isothermal solidification of a binary alloy, this is straightforward: re-writing Equ. (2) one has

$$\sigma^* = \frac{2\alpha d_{\mathrm{o}}}{\rho^2 V} = \frac{d_{\mathrm{o}}}{\rho Pt}\,(\text{thermal}) \qquad \text{or} \qquad \sigma^* = \frac{2Dd_{\mathrm{o}}}{\rho^2 V} = \frac{d_{\mathrm{o}}}{\rho Pc}\,(\text{solutal}) \tag{8}$$

where D is the solutal diffusivity and Pc is the solutal Peclet number ($Pc = V\rho/2D$, as distinct from the thermal Peclet number, Pt which has already been defined above). However, when both heat and solute are diffusing we should combine both Peclet numbers. Following the methodology suggested by [19] we write

$$\sigma^* = \frac{d_0}{\rho\left[\xi_{\mathrm{T}} Pt + 2\xi_c Pc \dfrac{|m|c_\infty}{L/c_p}\left(\dfrac{1-k_E}{1-(1-k_E)\Delta c}\right)\right]} \tag{9}$$

where Δc is the local concentration 'frozen in' at the interface (taken as $\phi = 0$) and which, like V and ρ, can be obtained directly from the phase-field simulation, thus providing a route for estimating σ^* in the coupled thermo-solutal case without recourse to the Ivantsov function. The value of σ^* thus obtained may be compared with that defined in the stability models proposed by Lipton, Glicksman & Kurz [3, 4] by setting $\xi_{\mathrm{T}} = \xi_{\mathrm{c}} = 1$ or to the model of Lipton, Kurz & Trivedi [5], by applying the high undercoolings corrections defined by

$$\xi_{\mathrm{T}} = 1 - \frac{1}{\sqrt{1 + \dfrac{1}{\sigma^* Pt^2}}} \quad , \quad \xi_c = 1 + \frac{2k_E}{1 - 2k_E - \sqrt{1 + \dfrac{1}{\sigma^* Pc^2}}} \tag{10}$$

Here we use the later of the two methodologies although, as described above, we would stress that this is for comparison purposes only and no recourse needs to be made to either the Ivantsov function nor to stability arguments to evaluate the right-hand sides of either Equ. (9) nor Equ. (10).

3. RESULTS

A number of sets of simulations have been conducted, in each case covering the (dimensionless) undercooling range $\Delta = 0.2 - 0.8$. Below $\Delta = 0.2$ we find that the growth velocity for the dendrite is so slow that excessive computation time is required in order to ensure that the dendrite has attained steady-state growth, while above $\Delta = 0.8$ the growth velocity becomes so large that it is no longer possible to ensure that the condition $W_0V/D < 1$ is satisfied [20], wherein the solution may no longer be independent of λ. The convergence behaviour of the model and the λ independence of the solutions has been studied by Ramirez & Beckermann [19] for an explicit solver and by Rosam et al. [21] for the implicit multigrid solver. In both cases the tests were conducted in the rapid solidification regime, with $\Delta = 0.55$. [19] expressed some concerns about convergence as they found that the velocity, Vd_0/α systematically increased by around 25 % as λ was increased from 1 to 4. Conversely [21] found that the superior convergence properties of the implicit multigrid solver resulted in much more robust predications as λ was increased. Specifically, as λ was increased from 1 to 4, Vd_0/α remained within a band of ±4% around its mean value (with the value at $\lambda = 1$ being within 1.25% of the value at $\lambda = 4$) while the Peclet number was constant to within ±2.5%. At the highest values of λ this corresponded to $W_0V/D \approx 0.8$, which gives us a reasonable degree of confidence in the convergence properties of the model in the rapid solidification regime.

The baseline parameter set for these simulations is given by $Le = 200$, $k_E = 0.3$, $Mc_\infty = 0.05$, $\lambda = 1$ and $\varepsilon = 0.02$. All simulations were run on a $[-1600:1600]^2$ domain with a minimum grid spacing of $h = 0.78$, equivalent, were a uniform mesh to have been used, of a mesh size which is $2^{12} \times 2^{12}$. From this starting point we have conducted three sets of simulations varying; Lewis number, Le, alloy concentration (via Mc_∞) and partition coefficient, k_E in turn, with all other parameters being held at the values given above.

The first parameter we consider is the Lewis number, which has been varied here over one order of magnitude, in the range $Le = 50$-500. Note that the Lewis number is varied by varying the thermal conductivity, α, with the solutal diffusivity, D, being kept constant during all simulations. This is as D also controls the coupling parameter, λ, via the relationship by $\lambda = D/a_2 = a_1 W_0/d_0$, which in turn sets the width of the diffuse interface.

The two main quantities which represent the direct output of the model are the dendrite tip velocity, V, and the radius of curvature at the dendrite tip, ρ. As described above, the radius of curvature reported here is the equivalent parabolic radius of curvature. Plots for the (dimensionless) velocity and radius of curvature as a function of undercooling, for $Le = 50$, 100, 200 & 500 are given in Figures 1 and 2 respectively.

In all cases the velocity increases monotonically with increasing undercooling showing, to a good approximation, a power law dependence, $V \propto \Delta^\beta$, with β being in the range 1.8-2.7. In fact this behaviour is much as we would expect. The analytical Ivantsov solutions for dendritic growth display this type of power-law behaviour for V in both 2- and 3-dimensions more-or-less independent of the assumptions made for the variation of ρ (i.e. marginal stability, growth at the extremum and even constant ρ appear to yield growth velocities displaying a power law dependence on Δ). Moreover, although experimental data [39, 40, 41, 42] is only available for free dendritic growth in 3-dimesions, experimental velocity-undercooling curves for a wide range of materials show a very similar type dependence.

There is a consistent trend for the growth velocity to increase with increasing Lewis number, which given that we control the Lewis number by adjusting the thermal diffusivity is to be expected.

The calculated (parabolic) tip radius, as determined from the phase-field model, as a function of undercooling is given in Fig. 2. This may be compared (Fig. 3) with that which would be expected from the LKT [5] marginal stability model with the same input parameter set and a constant stability parameter σ^*, the value of which is taken here as 0.05. In all cases the tip radius as determined from the phase-field model passes through a local minimum as the undercooling is increased, although at low Lewis number this minimum is very poorly developed. The undercooling at which the minimum occurs moves systematically to lower undercoolings as the Lewis number is increased, from a value of $\Delta = 0.75$ at Lewis number 50 to $\Delta = 0.28$ at Lewis number 500. This behaviour is, at least qualitatively, in agreement with marginal stability type models. However, the marginal stability model predicts that in addition to a local minimum the tip radius should also display a local maximum at yet higher undercooling, after which the tip radius declines steadily with increasing undercooling. This behaviour is not observed in any of the phase-field simulations, with the radius increasing steadily with undercooling in the high undercooling regime at all Lewis numbers. In deed, at $Le = 500$ the tip radius at $\Delta = 0.8$ exceeds that at $\Delta = 0.2$ by a factor of 2, clearly at variance with marginal stability models.

The dependence of the dendrite tip radius upon undercooling as predicted by marginal stability type models, with its characteristic local minimum followed by a local maximum, has very much been a cornerstone of rapid solidification theory for the past 20 years. However, experimental evidence in support of the existence of either a local minimum, or a local maximum, in the tip radius is scant. Transparent analogue casting alloys, such as succinonitrile-acetone, in which direct measurement of the dendrite tip radius is possible [24],

can only be undercooled by very small amounts so that the predicted undercooling range in which a local minimum might be observed is not accessible. In metallic systems only an indirect estimate of the tip radius is possible, generally by assuming that some characteristic microstructural length scale, such as the grain size or dendrite trunk radius where observable [43], scales as a constant multiple of the tip radius. However, although there is plentiful evidence of an initial decrease in microstructural length scale in the low undercooling region, it has proved almost impossible to make a continuous extension of such an analysis into the high undercooling regime where the presence of a local minimum might be inferred. Even for systems where a single dendritic phase exists over the whole undercooling range, such as Ni-Cu [39] or Cu-O [44], the intervention of remelting and/or recrystallisation effects such as spontaneous grain refinement [43, 45, 46] make the estimation of the original tip radius during dendritic growth impossible. Given that the local minimum in the tip radius moves to lower undercooling as the Lewis number is increasing we consider, on the balance of probabilities, that at higher Lewis numbers than those studied here it may still be the case that a local maximum in the tip radius will be observed. However, from the results presented here we conclude that the occurrence of such maxima is nowhere near as ubiquitous as suggested by marginal stability models.

The estimated value of the effective stability parameter, σ^*, as estimated from the phase-field results is shown in Fig. 4. For all Lewis numbers studied the results show that as the undercooling is increased, σ^* shows first a local minimum, followed by a local maximum. The location of both this minima and maxima shift to lower undercooling as the Lewis number is increased and moreover, the amplitude of the variation between the maximum and minimum value also increases with Lewis number. In fact we note that if we were to make a qualitative comparison, considering only the general shapes of the curves, there is a far greater similarity between the marginal stability curve for the radius, calculated

on the basis of constant σ^*, and the dependence predicted here for the stability parameter, σ^*, than there is between the marginal stability curve and the actual tip radius predicted by the phase-field model. Of course, given that we are comparing dissimilar quantities this can only be a purely qualitative comparison, yet the similarity in form is striking. A discussion of the potential significance of this result is reserved for later, we first consider the effect of alloy concentration and partition coefficient.

The velocity data as a function of Mc_∞ in the range $Mc_\infty = 0.02$-0.10 is given in Figure 5. Again we observe a power law dependence between the velocity and undercooling, although now with a much narrower range of exponents (2.3-2.6). As might be expected dendrites of the most dilute alloy grow most rapidly, with the solidification velocity showing a systematic decrease as the alloy becomes more concentrated. The corresponding dendrite tip radius data is shown in Figure 6. For the most part, at fixed undercooling the radius appears to be largest in the most dilute alloys and to decrease with increasing concentration, although the curves for $Mc_\infty = 0.02$ and $Mc_\infty = 0.035$ cross at $\Delta = 0.65$ so that at very high undercooling the largest dendrites grow at $Mc_\infty = 0.035$. For all values of Mc_∞ studied a local minimum in the tip radius is observed while, as in Fig. 2, none of the curves show a local maximum, which is again at variance with the prediction of the LKT marginal stability model operating with the same parameters set and a fixed value of σ^* (see Fig. 7). In deed, the correspondence between the predictions of the LKT theory and those of the phase-field model is even weaker than was the case with the variation of Lewis number. LKT theory predicts that the local minimum in the tip radius should move to progressively higher undercoolings as the concentration is increased, whereas in the phase-field model the local minimum occurs at the highest undercoolings in both the most dilute and the most concentrated alloys, with intermediate concentrations giving rise to local minima at lower undercoolings. Moreover, the LKT radius curves display a distinct, well defined minimum

followed by an equally well defined maximum. In contrast, for all concentration except $Mc_\infty = 0.02$, the phase-field model displays a broad range of intermediate undercoolings over which the radius is almost constant. The data for $Mc_\infty = 0.035$ is a case in point, with the radius showing a variation of no more than 13% over the undercooling range $\Delta = 0.3250 - 0.6875$. However, if we now consider the equivalent values of the effective stability constant, σ^*, recovered from the phase-field model (Fig. 8), we again see a remarkable qualitative similarity with the radius curves generated from the marginal stability model. In particular, all the curves display a minimum which shifts systematically to higher undercooling as the concentration is increased. Moreover, with the exception of the most concentrated alloy, in which the minimum does not occur until $\Delta = 0.725$, all curves display a maximum, which similarly shifts to higher undercooling as the concentration is increased.

Finally we consider the case of varying the partition coefficient, k_E, two values of which have been studied, 0.3 and 0.15. For (isothermal) solute only simulations both V and ρ (and hence Pc and σ^*) are independent of k_E. This result is well known from the literature and is reproduced by our models (reduction of the coupled thermo-solutal model to solute only is discussed in both [19] and [21]), with validation of the independence from k_E being demonstrated for a solutal undercooling of 0.4 and for k_E = 0.01, 0.02, 0.05, 0.1, 0.3. No more than a 1% variation in either V or ρ was observed. However, this is not the case in coupled thermo-solutal model in which changing the value of k_E alters the relative influence of thermal and solutal control on the growth (the dominant effect appears to be for the higher solute concentration at the tip to give rise to a tip of smaller radius).

The velocity-undercooling curves for these two simulations are shown in Fig. 9. At low undercoolings ($\Delta < 0.4$) there is very little difference between the calculated growth velocities for each case, although above an undercooling of 0.4 the more strongly partitioning system displays a systematically higher growth velocity (due to the higher curvature of the tip). As

previously, the velocity-undercooling relationship is approximated well by a simple power law, with the exponents being 2.3 and 2.7 for $k_E = 0.3$ and 0.15 respectively. The radius of curvature at the tip, as calculated from the phase-field model, is shown in Fig. 10, and may be compared with the equivalent LKT marginal stability calculation, which is shown in Fig. 11. As discussed above the agreement in the case of $k_E = 0.3$ is poor, with the phase-field model displaying a local minimum, but not a maximum in the tip radius. In the case of $k_E = 0.15$ the agreement is rather better, although this is probably due to the fact that in the more strongly partitioning system the marginal stability model also displays only a minimum tip radius and no maximum (within the undercooling range studied). In both the marginal stability and phase-field models it is also the case that the undercooling at which the minimum occurs is shifted to higher values in the more strongly partitioning system. The effective value of the stability parameter, σ^*, estimated from the phase-field model is shown in Fig. 12. The close correspondence between the phase-field σ^* curve and the marginal stability curve for ρ in the case of $k_E = 0.3$ has been noted above. In the case of $k_E = 0.15$ the agreement is less good. The LKT radius curve shows a very shallow minimum towards top of the undercooling range studied, whereas the phase-field σ^* curve decreases monotonically over the whole of the undercooling range studied. We do however note that marginal stability predicts that there should be essentially no dependence upon partition coefficient at low undercoolings ($\Delta < 0.4$), a trend that is replicated in the phase-field data for σ^* but not for ρ.

4. DISCUSSION

We have presented evidence above that suggests if we use a phase-field model of coupled thermo-solutal growth formulated in the thin-interface limit to calculate the radius of curvature at the tip of a dendrite growing at high undercooling into its parent melt, poor correspondence is obtained with the much simpler LKT model based on the ideas of marginal

stability. This is hardly surprising as there is an extensive body of evidence in the literature that suggests that at high undercooling σ^* is very far from being constant. Perhaps one of the most important results to highlight from this study is that although all of our radius curves display a local minimum as the undercooling is increased, none display a local maximum. The idea of the local minimum followed by local maximum in the tip radius has become common currency within the rapid solidification community, possibly mistakenly so.

What may be more surprising is that if we make a qualitative comparison, many of the trends observed in the marginal stability radius curves are reproduced in the phase-field curves for σ^*. Below we discuss this similarity. We draw the analogy between σ^* for the phase-field model and radius for the marginal stability model, not because we ascribe any particular validity to the ideas of the marginal stability model, we do not, but because in the case of an analytical model it is easier to understand where affects may arise in a way that is not always the case in a numerical model. Thus the analogy is to aid the interpretation of the phase-field results and to attempt to elicit a physical understanding which might otherwise be difficult to extract from equations that can, by their nature, only be solved numerically.

To begin to understand this similarity we first consider the rather simpler case of growth with just a single diffusing species, in this case heat, as a dendrite of a pure material grows into its undercooled parent melt. By simply setting the concentration parameter, Mc_∞, to zero the same phase-field model as described above can be used to simulate growth in this system, albeit in perhaps not the most computationally efficient manner. The calculated value of σ^* resulting from performing a set of such simulations is shown in Fig. 13. The equivalent marginal stability calculation of the tip radius for a system under thermal only control is shown in Fig. 14. The two curves display a superficial resemblance in that both show a steady, monotonic decrease as the undercooling is increased, although this is far steeper in the case of the marginal stability radius than for σ^* from the phase-field model. Both curves

accord closely with what might be expected from other work in the literature. Similar profiles would be expected if we were to repeat this as a solute only calculation, although for brevity this is not reproduced here. Moreover, in the case of the marginal stability calculation of the tip radius it is well understood how two similar curves, each showing a monotonic decrease, but for different species (heat and solute) diffusing over very different length and time scales can give rise to the characteristic alloy curve (e.g Figs. 3, 7, 11) which show both a local minimum and a local maximum. The initial, low undercooling, region of the curve is the result of the dendrite growing, at least to a first approximation, under solute only control, with the decrease in ρ being the result of increasing solutal Peclet number. At intermediate undercoolings we have high solutal but low thermal Peclet numbers and growth control begins to be transferred to thermal diffusion, with a commensurate increase in ρ. Finally, at high undercooling, the effect of solute diffusion on the growth becomes negligible and thermal diffusion becomes the dominant process controlling growth. The radius increase that was observed as control moves to thermal diffusion is reversed, leading to a local maximum in the radius followed by a steady decline as growth moves into the high thermal Peclet number regime. The exact details of where these transitions occur and the balance of thermal versus solutal control depend upon the details of the model assumed and the material parameters for the system being considered, although the gross features are independent of the mathematical model.

Of course, all of this assumes constant σ^*. If we now consider the case in which σ^* is not constant we may apply a similar argument, but now applied to the selection parameter σ^*, rather than the tip radius *per se*. Consequently, it will be σ^* that show the characteristic local minimum followed by local maximum as the undercooling is increased. If we then accept that it is σ^* and not tip radius directly that is determined by the competition between thermal and solutal transport processes as the dendrite grows, we can now begin to understand why

The above hypothesis is presented as an argument which, at least qualitatively, allows the results of the phase-field simulation to be rationalised. We have not attempted to put a mathematical framework around these arguments and, indeed, do not know whether such a framework would be possible. However, if it *were* possible to combine σ^* curves calculated separately for thermally and solutally controlled growth within an appropriate mathematical framework this would offer the intriguing possibility that σ^* (and hence characteristic length scales and growth velocities) for a dendrite growing under coupled thermo-solutal control may be *estimated* without performing simulations on the particular system being considered.

5. REFERENCES

1. G. P. Ivantsov, Doklady Akademii Nauk SSSR **58,** 567 (1957).
2. W. W. Mullins and R. F. Sekerka, J. Appl. Phys. **33**, 444 (1964).
3. J. Lipton, M. E. Glicksman and W. Kurz, Mater. Sci. Eng. **65**, 57 (1984).
4. J. Lipton, M. E. Glicksman and W. Kurz, Metall. Trans. A **18**, 341 (1987).
5. J. Lipton, W. Kurz and R. Trivedi, Acta Metall. **35**, 957 (1987).

6. R. Willnecker, D. M. Herlach and B. Feuerbacher, Phys. Rev. Lett. **62**, 2707 (1989).
7. S. C. Huang and M. E. Glicksman, Acta Metall. **29**, 701 (1981).
8. E. Ben-Jacob, N. D. Goldenfeld, B. G. Kotliar and J. S. Langer, Phys. Rev. Lett. **53**, 2110 (1984).
9. J. S. Langer, Phys. Rev. A **33**, 435 (1986).
10. A. M. Mullis, R. F. Cochrane, Acta Mater. **49**, 2205 (2001).
11. J. S. Langer, in *Directions in condensed matter physics*, edited by G. Grinstein and G. Mazenko G., pp. 164-186 (World Science 1986).
12. G. Caginalp, Phys. Rev. A **39**, 5887 (1989).
13. O. Penrose and P. C. Fife, Physica D **43**, 44 (1990).
14. A. Karma and W. J. Rappel, Phys. Rev. E **53**, R3017 (1996).
15. A. Karma and W. J. Rappel, J. Cryst. Growth **174**, 54 (1997).
16. A. Karma and W. J. Rappel, Phys. Rev. E **57**, 4323 (1998).
17. D. A. Kessler, J. Koplik and H. Levine, Adv. Phys. **37**, 255 (1988).
18. Y. Pomeau and M. Ben-Amar, in *Solids far from equilibrium* pp. 365-431 (Cambridge University Press 1992).
19. J. C. Ramirez and C. Beckermann, Acta Mater. **53**, 1721 (2005).
20. J. C. Ramirez and C. Beckermann, Phys. Rev. E **69**, 051607 (2004).
21. J. Rosam, P. K. Jimack and A. M. Mullis, Acta. Mater. **56**, 4559 (2008).
22. J. Rosam, P. K. Jimack and A. M. Mullis, Phys. Rev. E **79**, 030601 (2009).
23. Q. Li and C. Beckermann, J. Cryst. Growth **236**, 482 (2002).
24. M. A. Chopra, M. E. Glicksman and N. B. Singh, Metall. Trans. A **19**, 3087 (1988).
25. M. Rebow and D. J. Browne, Scripta Mater. **56**, 481 (2007).
26. Ch-A. Gandin and M. Rappaz, Acta Mater. **42**, 2233 (1994).
27. M. A. Martorano and V. B. Biscuola, Modell Simul Mater. Sci. Eng. **14**, 1225 (2006).

28. D. J. Browne and J. D. Hunt, Numer. Heat Transfer B **45**, 395 (2004).
29. C. Y. Wang and C. Beckermann, Metall Mater. Trans. A **25**, 1081 (1994).
30. M. A. Martorano, C. Beckermann and Ch-A. Gandin, Metall Mater. Trans. A **34**, 1657 (2003).
31. A. I. Ciobanas, Y. Fautrelle, F. Batraretu, A. M. Bianchi and A. Noppel, in *Modelling of Casting Welding & Advanced Solidification Processing XI*, edited by Ch-A. Gandin and M. Bellet, pp. 299-306 (TMS Warrendale PA 2006).
32. A. Karma, Phys. Rev. Lett. **87**, 115701 (2001).
33. A. M. Mullis, Comp. Mater. Sci. **36**, 345 (2006).
34. J. Rosam, *A fully implicit, fully adaptive multigrid method for multi-scale phase-field modelling*, Ph.D. thesis (University of Leeds 2007).
35. U. Trottenberg, C. Oosterlee and A. Schuller, *Multigrid* (Academic Press 2001).
36. A. Brandt, Math. Comp. **31**, 333 (1977).
37. J. Rosam, P. Jimack and A. Mullis, J. Comp. Phys. **225**, 1271 (2007).
38. X. Tong, C. Beckermann, A. Karma and Q. Li, Phys. Rev. E **63**, R49 (2001).
39. R. Willnecker, D. M. Herlach and B. Feuerbacher, Phys. Rev. Lett. **62**, 2707 (1989).
40. B. T. Bassler, W. H. Hofmeister, G. Carro and R. J. Bayuzick, Metall. Mater. Trans. **25**, 1301 (1994).
41. S. E. Battersby, R. F. Cochrane and A. M. Mullis, Mater. Sci. Eng. A **226**, 443 (1997).
42. K. Dragnevski, R. F. Cochrane and A. M. Mullis, Phys. Rev. Lett. **89**, 215502 (2002).
43. M. Schwarz, A. Karma, K. Eckler and D. M. Herlach, Phys. Rev. Lett. **73**, 1380 (1994).
44. S. E. Battersby, R. F. Cochrane and A. M. Mullis, J. Mater. Sci. **35**, 1365 (2000).
45. A. M. Mullis, Int. J. Heat Mass Trasfer **40**, 4085 (1997).
46. K. Dragnevski, R. F. Cochrane and A. M. Mullis, Mater. Sci. Eng. A **375-377**, 479 (2004).

6. FIGURES

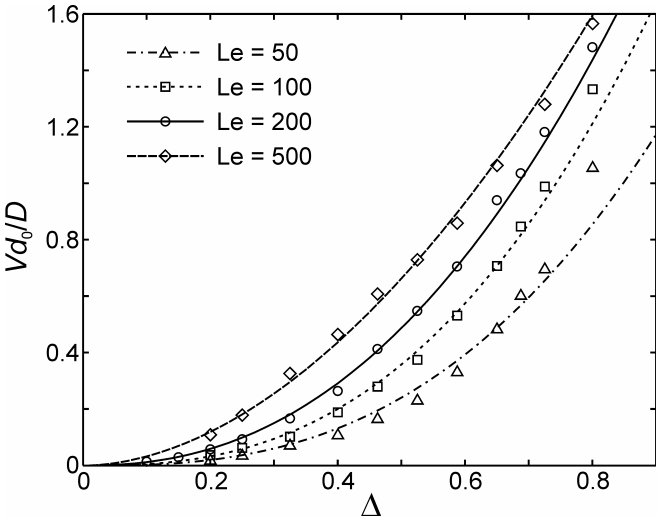

Fig. 1. Dendrite growth velocity as a function of undercooling, as calculated by the coupled thermo-solutal phase-field model, for dendrites growing at varying Lewis number.

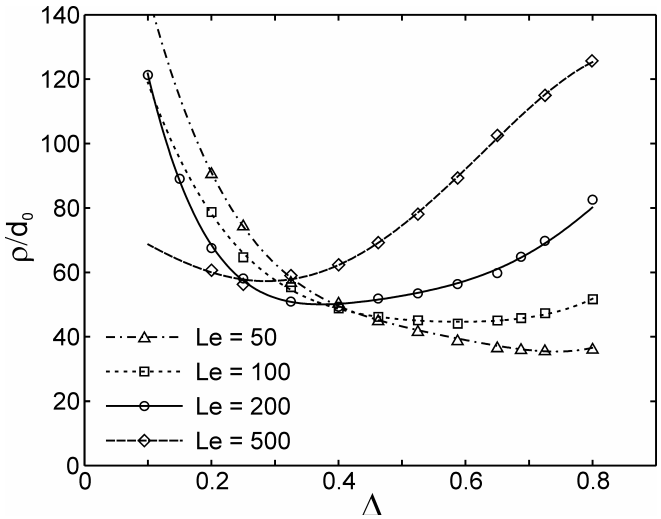

Fig. 2. Radius of curvature at the dendrite tip as a function of undercooling, as calculated by the coupled thermo-solutal phase-field model, for dendrites growing at varying Lewis number.

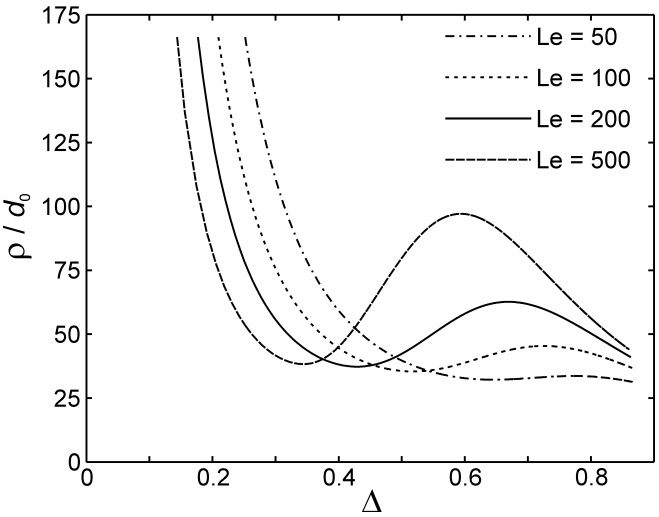

Fig. 3. Radius of curvature at the dendrite tip as a function of undercooling as predicted by marginal stability (LKT) theory on the assumption of constant stability parameter, σ*. Growth parameters are the same as used in the phase-field model.

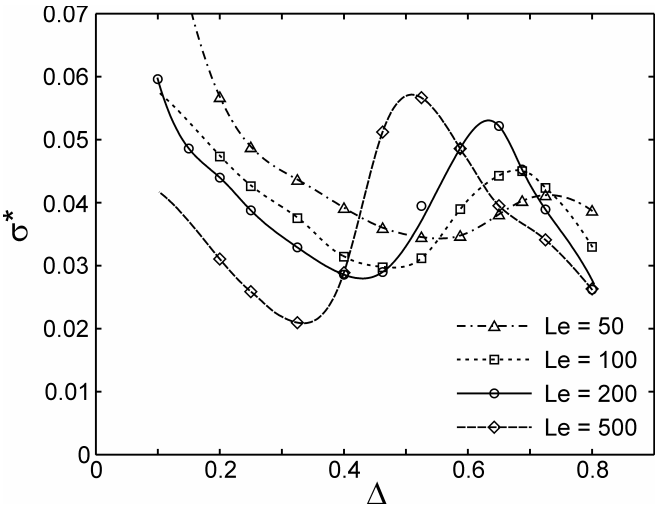

Fig. 4. Values of the effective stability parameter σ* as a function of undercooling, as calculated by the coupled thermo-solutal phase-field model, for dendrites growing at varying Lewis number.

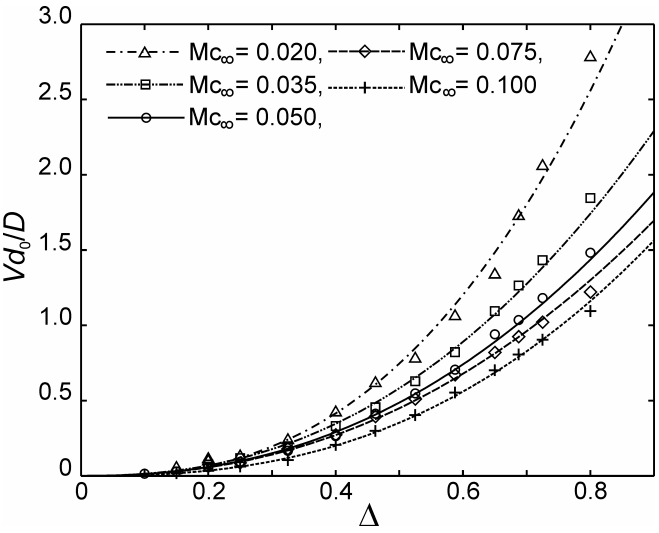

Fig. 5. Dendrite growth velocity as a function of undercooling, as calculated by the coupled thermo-solutal phase-field model, for dendrites growing at varying solute concentrations.

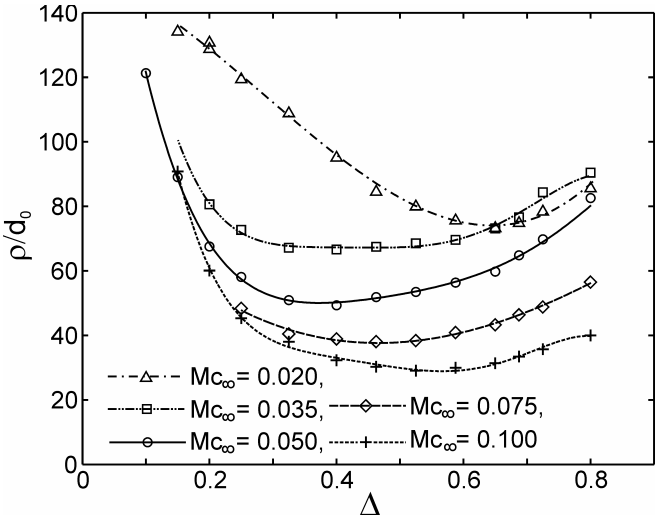

Fig. 6. Radius of curvature at the dendrite tip as a function of undercooling, as calculated by the coupled thermo-solutal phase-field model, for dendrites growing at varying solute concentrations.

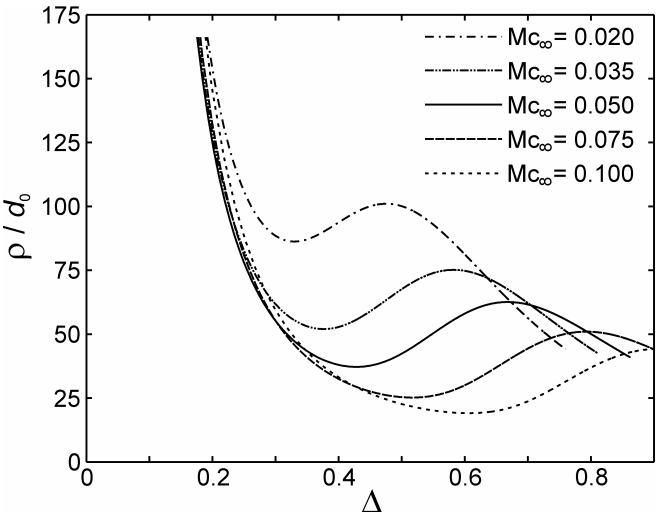

Fig. 7. Radius of curvature at the dendrite tip as a function of undercooling as predicted by marginal stability (LKT) theory on the assumption of constant stability parameter, σ*. Growth parameters are the same as used in the phase-field model.

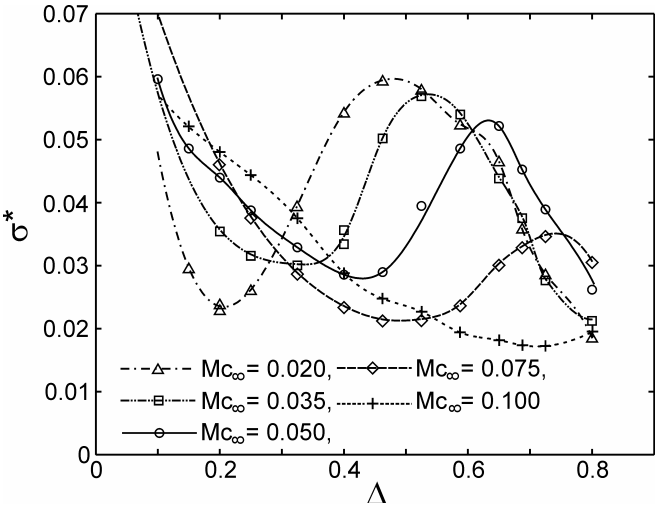

Fig. 8. Values of the effective stability parameter σ* as a function of undercooling, as calculated by the coupled thermo-solutal phase-field model, for dendrites growing at varying solute concentrations.

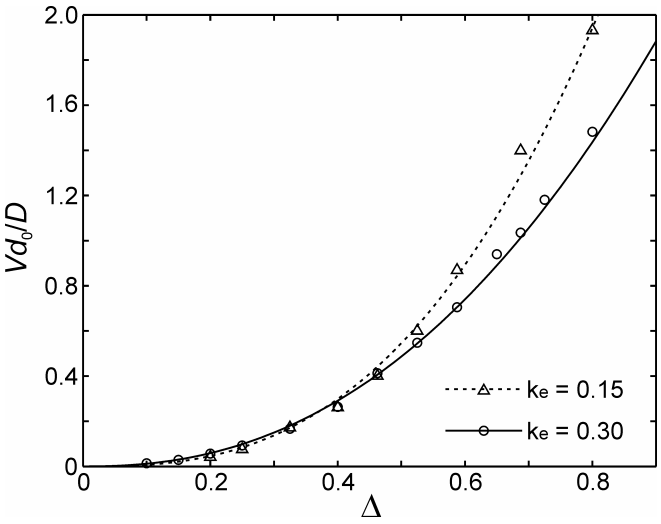

Fig. 9. Dendrite growth velocity as a function of undercooling, as calculated by the coupled thermo-solutal phase-field model, for dendrites growing at varying partition coefficient.

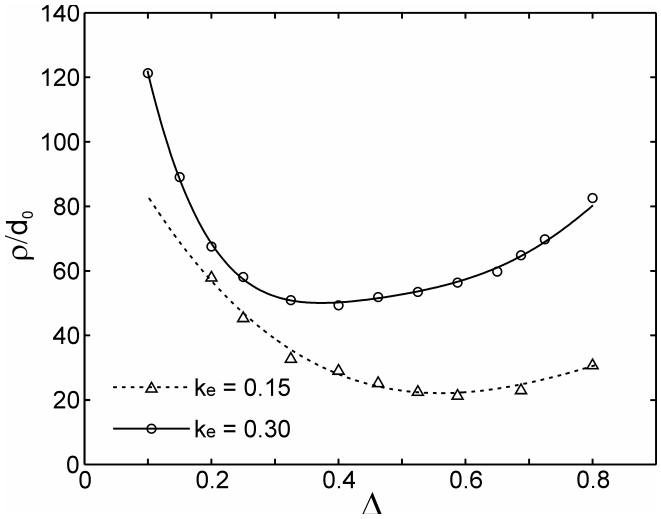

Fig. 10. Radius of curvature at the dendrite tip as a function of undercooling, as calculated by the coupled thermo-solutal phase-field model, for dendrites growing at varying partition coefficient.

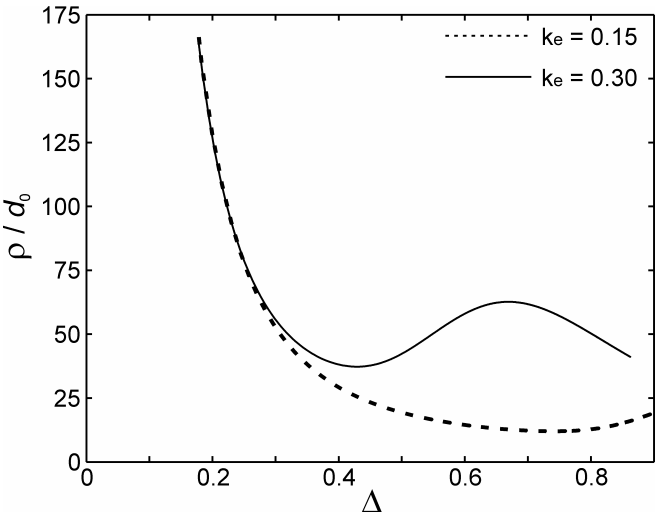

Fig. 11. Radius of curvature at the dendrite tip as a function of undercooling as predicted by marginal stability (LKT) theory on the assumption of constant stability parameter, σ*. Growth parameters are the same as used in the phase-field model.

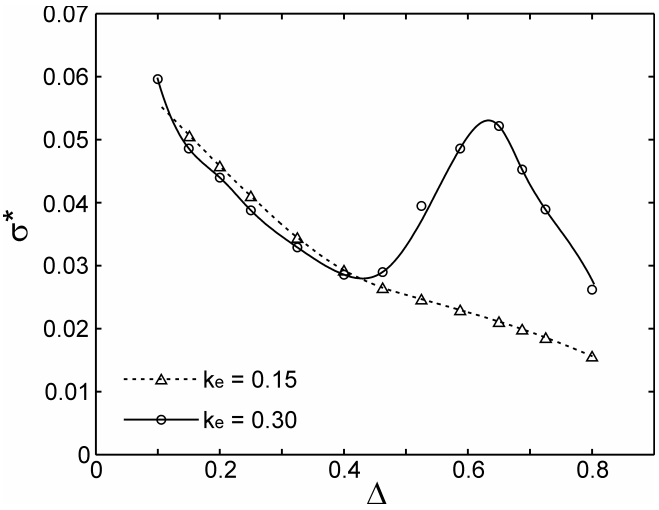

Fig. 12. Values of the effective stability parameter σ* as a function of undercooling, as calculated by the coupled thermo-solutal phase-field model, for dendrites growing at varying partition coefficient.

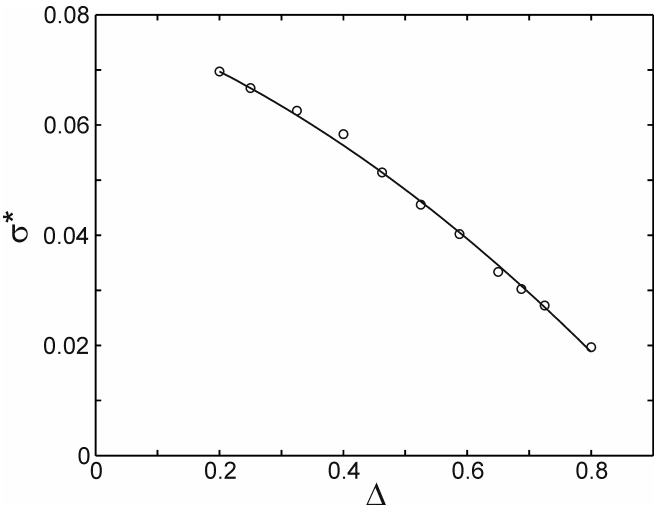

Fig. 13. Value of the effective stability parameter σ* as a function of undercooling, as calculated by the phase-field model, for a dendrite growing under thermal only control.

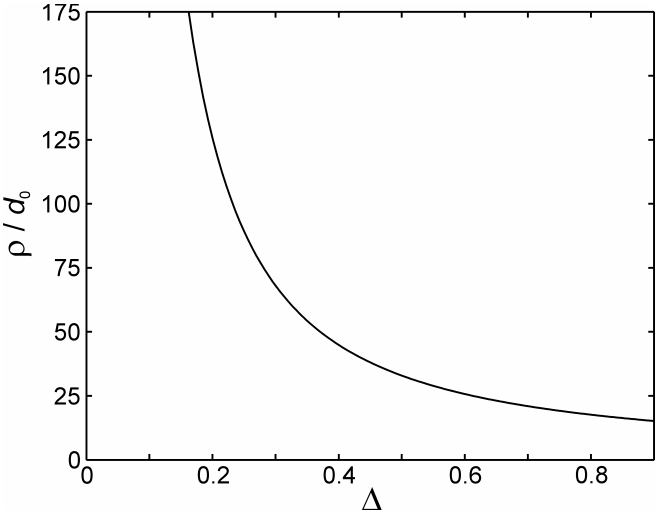

Fig. 14. Radius of curvature at the dendrite tip as a function of undercooling as predicted by marginal stability (LKT) theory on the assumption of constant stability parameter, σ*, for a dendrite growing under thermal only control.